A state space model for real-time control of the temperature in indoor space - Principle, calibration and results

Alain Sempey, Christian Inard, Cristian Ghiaus, Cyrille Allery

A state space model for real-time control of the temperature in indoor space: principle, calibration and results

A. Sempey[1], C. Inard[1], C. Ghiaus[2] and C. Allery[1]

[1]Laboratoire d'étude des phénomènes de transfert appliqués au bâtiment (LEPTAB), Université de La Rochelle, avenue Michel Crépeau, 17042 La Rochelle cedex 1, France
[2]Centre Thermique de Lyon (CETHIL) UMR 5008, INSA Lyon, 9, rue de la Physique, 69621 Villeurbanne cedex, France

Abstract

Real-time control of comfort in indoor spaces needs models of temperature distribution and air velocity field. Complete models, based on CFD, give this information but are improper for real-time calculations. Therefore, a reduced model is needed. This study proposes to reduce the dimension of a CFD model by first considering the velocity field fixed and solving only the energy balance equation, then putting this equation in the form of state-space and finally by reducing its order by Proper Orthogonal Decomposition (POD). This article focuses on the correction of the reduced order model which is absolutely necessary before using it for real time application. This algorithm was applied to a room equipped with a fan coil with an air jet having three patterns: sticking to the ceiling and reaching the opposite wall, falling before the opposite wall, and falling before reaching the ceiling. For the two-dimensional case, the reduced model has been validated by comparison with CFD results for step inputs of temperature and air velocity. As the order of the reduced model is always smaller than 7, the energy balance equation may be solved in real time and integrated into a control algorithm.

Key words: Simulation, POD, energy, temperature, velocity, state space, reduced order.

Nomenclature

a_{eff}	effective air diffusivity (m^2/s)
$a_n(t)$	temporal coefficient, computed with the reduced order model, associated to the n^{th} eigenfunction
$\mathbf{a}(t)$	vector of temporal coefficient
$\tilde{\mathbf{a}}(t)$	vector of Lagrange multipliers
$b_n(t)$	temporal coefficient extracted from the snapshot, associated to the n^{th} eigenfunction
C_p	specific heat at constant pressure (J/kg°C)
E	mean energy
J	cost functional
L	Lagrangian
M	number of snapshot
m	number of eigenfunctions
N	constraints
n_θ	number of data for the Rmse calculation
$Rmse$	root mean square error (°C)
S_p	source power (W/m^3)
t	time (s)
$\mathbf{v}$	velocity field (m/s)
$\mathbf{x}$	space coordinates

Greek letters

$\boldsymbol{\alpha}$	coefficients of calibration
θ	air temperature (°C)
λ	eigenvalue
ρ	air density (kg/m^3)
ϕ	eigenfunctions

Subscripts

d	diffusive term
m	mean quantity
n	number of the eigenvector
r	reduced order matrix
t	transport term
ref	reference data

1. Introduction

In air conditioning spaces, the air velocity field and the temperature distribution are not uniform, with implications on thermal comfort and energy consumption. Generally, this characteristic is not taken into account by the control system. Even though computational fluid dynamics (CFD) may predict the temperature distribution and the velocity field, computing time is prohibitive for real time control. For the problem of indoor air flow, Peng (Peng 1996) proposed to calculate the dynamic temperature distribution in a fixed flow field, provided that it is correctly calculated by the CFD code. So in this paper, only the energy balance equation needs to be solved. We propose the reduction of this equation by using Proper Orthogonal Decomposition. This technique is based on the construction of an optimal basis-function which contains enough information for an accurate description of the temperature distribution.

This article briefly describes the method of construction of a high order state space model based on the assumption of a fixed velocity field, and the subsequent implementation of the POD to get a reduced order state space model. Emphasis will be placed on the method used for correction of the reduced order model based on solving an optimization problem under constraint. The CFD simulations performed prior are considered as reference data, and are used to validate models

2. Theory

2.1 Reduced order model

The energy balance is described by the differential equation:

$$\frac{\partial \theta}{\partial t} + \mathbf{v} \bullet \mathbf{grad}\,\theta = div\left(a_{eff}\,\mathbf{grad}\,\theta\right) + \frac{S_p}{\rho C_p} \qquad (1)$$

Provided that the flow field can be correctly calculated by a CFD code, Ghiaus and Ghiaus (Ghiaus et al 1999) show how to obtain a state space form after discretization. This is a more advantageous representation for control, in which the temperatures are written in a vector. The high order model is then:

$$\begin{cases} \dot{\boldsymbol{\theta}} = \mathbf{A}\boldsymbol{\theta} + \mathbf{B}\mathbf{u} \\ \mathbf{y} = \mathbf{C}\boldsymbol{\theta} + \mathbf{D}\mathbf{u} \end{cases} \text{with } \dot{\boldsymbol{\theta}} = \frac{d\boldsymbol{\theta}}{dt}\,, \qquad (2)$$

where $\boldsymbol{\theta}$ is the state vector, $\mathbf{u}$ the input vector, $\mathbf{y}$ the output vector, $\mathbf{A}$ the state matrix, $\mathbf{B}$ and $\mathbf{D}$ input matrix and $\mathbf{C}$ the output matrix. For each fixed air-flow pattern, the system (2) gives the air temperature distribution in all the room. The size of the first equation is exactly equal to the number of discretization cells for CFD calculations.

The order of system (2) is too high to be used in real-time applications. A reduction of the order can be achieved by finding an optimal basis with the Proper Orthogonal Decomposition (POD), (Allery et al 2005) and (Gunes 2002). This method needs *M* snapshots extracted from a transient simulation made with the CFD. The basic idea of the POD consists in finding a ‘‘physical’’ basis which is optimal in an energetic sense. Thus, we search a deterministic function, ϕ, which gives the ‘‘best’’ representation of the set of temperature. From variational calculus, it follows that this problem is equivalent to an eigenvalue problem. In order to reduce the calculation, we used the snapshots method (Sirovich 1987) which leads to the following expression of temperature:

$$\theta(\mathbf{x},t) = \theta_m(\mathbf{x}) + \sum_{i=1}^{M} b_i(t)\phi_i(\mathbf{x}) \qquad (3)$$

where θ_m is the mean temperature.

Owing to the propriety of the eigenvalue problem, eigenvalues are real and non-negative and can be ordered as $\lambda_1 \geq \lambda_2 \Lambda \geq \lambda_M$. Each eigenvalue λ_n, taken individually, represents the energy contribution of the corresponding eigenfunction. The eigenvectors ϕ_i satisfy the boundary conditions and can be normalized to form an orthonormal set. The

main property of the POD is its ability to give the best approximation of the distribution in an energetic sense. The energy contained in the first *m* modes is indeed always greater than the energy contained in any other basis, such as the Fourier basis. If POD is applied to the velocity field, this energy is related to the fluid's kinetic energy. In the case of a temperature distribution, the fact that a mode captures, for instance, 65% of the energy means in a probabilistic sense that the system spends 65% of its time executing this mode (Deane et al 1991). Then, by keeping only the first *m* modes and ignoring the remaining modes, the temperature is written as:

$$\theta(\mathbf{x},t) \approx \theta_m(\mathbf{x}) + \sum_{i=1}^{m} b_i(t)\phi_i(\mathbf{x}) \tag{4}$$

The number of basis functions is chosen according to an energetic criterion which ensures the conservation of maximum energy:

$$E = \frac{\sum_{i=1}^{m}\lambda_i}{\sum_{i=1}^{M}\lambda_i} \geq 90\% \; and \; \frac{\lambda_m}{\lambda_1} \leq 10^{-2} \tag{5}$$

Only a very small number m of functions are sufficient to rebuild the temperature distribution. In order to obtain a low dimensional model, equation 4 is substituted into equation 2 and after a change of variable leads to a state space system of order *m*:

$$\begin{cases} \dot{\mathbf{a}} = \mathbf{A_r}\mathbf{a} + \mathbf{B_r}\mathbf{u} \\ \boldsymbol{\theta} = \mathbf{C_r}\mathbf{a} + \mathbf{D_r}\mathbf{u} \end{cases} \tag{6}$$

The low order model 6 gives the behaviour of coefficients $\mathbf{a} = (a_i)_{i\in[1\,m]}$ as a function of the input vector. Knowing the basis functions ϕ_i, the temperature is then rebuilt with use of the expression 4, leading to the second equation of model 6.

2.2 State calibration method

Although very few POD modes contain most of the energy and can be kept to construct a reduced-order dynamical system, the low-energetic modes, which drop out, must be taken into account to recover an accurate description of the temperature. Most authors use a diffusive model based on the Heisenberg spectral viscosity model (Allery 2002; Couplet et al 2003; Podvin et al 2001; Rempfer 1994). The effect of the low-energetic modes on the high-energetic modes is then equivalent to the increase of dissipation. In practice, an artificial viscosity is added to the state equation. First, it is more convenient to separate the first equation of the system 6 into a diffusive part and a transport part issued from the corresponding terms of the equation 1.

$$\dot{\mathbf{a}} = (\mathbf{A_{rt}} + \mathbf{A_{rd}})\mathbf{a} + (\mathbf{B_{rt}} + \mathbf{B_{rd}})\mathbf{u} \tag{7}$$

Then, the addition of the artificial viscosity is equivalent to the increase of the diffusivity by $\alpha_j a_{eff}$ and leads to the new state equation:

$$\dot{\mathbf{a}} = \mathbf{A_{rt}}\mathbf{a} + \mathbf{B_{rt}}\mathbf{u} + \mathbf{I}_{1+\alpha}(\mathbf{A_{rd}}\mathbf{a} + \mathbf{B_{rd}}\mathbf{u}) \tag{8}$$

Where $\mathbf{I}_{1+\alpha}$ is a diagonal matrix given by:

$$\mathbf{I}_{1+\alpha} = \begin{pmatrix} 1+\alpha_1 & & 0 \\ & \mathrm{O} & \\ & & \mathrm{O} \\ 0 & & 1+\alpha_m \end{pmatrix} \tag{9}$$

Here, the state space form turns out to be very interesting as it gives access to the modern control theory. Indeed, the calibration aims at approaching the coefficients b_i by the coefficients a_i. So, an attractive element of the optimal control theory is the introduction of a cost functional which provides a quantitative measure of this objective:

$$J(\mathbf{a},\boldsymbol{\alpha}) = \int_0^T \sum_{j=1}^{m} (a_j - b_j)^2 dt + \beta \int_0^T \sum_{j=1}^{m} \alpha_j^2 dt \tag{10}$$

The second term represents the cost link to the difference between the effective diffusivity a_{eff} and the corrected diffusivity $(1+\alpha_j)a_{eff}$. The calibration problem is then expressed as:

$$\begin{cases} \min_{\boldsymbol{\alpha}} J(\mathbf{a},\boldsymbol{\alpha}) \\ subject\ to \\ N(\mathbf{a},\boldsymbol{\alpha}) = 0 \end{cases} \tag{11}$$

where the constraints $N(\mathbf{a},\boldsymbol{\alpha})=0$ correspond to the equation 8. The constrained optimization problem 11 is solved using the Lagrange multiplier method. The constraints are enforced by introducing the Lagrange multipliers or adjoint variables $\tilde{\mathbf{a}}$ and the Lagrangian functional:

$$\begin{aligned} L(\mathbf{a},\boldsymbol{\alpha},\tilde{\mathbf{a}}) &= J(\mathbf{a},\boldsymbol{\alpha}) - \left\langle N(\mathbf{a},\boldsymbol{\alpha}),\tilde{\mathbf{a}}\right\rangle \\ &= J(\mathbf{a},\boldsymbol{\alpha}) - \sum_{j=1}^{n}\int \tilde{\mathbf{a}}_j N_j(\mathbf{a},\boldsymbol{\alpha})dt \end{aligned} \quad (12)$$

The solutions (state $\mathbf{a}$, co-state $\tilde{\mathbf{a}}$ and coefficient of calibration $\boldsymbol{\alpha}$) of this new unconstrained optimization problem are such that is rendered stationary:

$$\delta L = \frac{\partial L}{\partial \mathbf{a}}\delta\mathbf{a} + \frac{\partial L}{\partial \boldsymbol{\alpha}}\delta\boldsymbol{\alpha} + \frac{\partial L}{\partial \tilde{\mathbf{a}}}\delta\tilde{\mathbf{a}} = 0 \quad (13)$$

where $\partial\mathbf{a}$, $\partial\boldsymbol{\alpha}$ and $\partial\tilde{\mathbf{a}}$ are arbitrary variations. Considering that each argument of L is independent of the others, the calibration problem is determined by setting the first variation of L with respect to $\tilde{\mathbf{a}}$, $\mathbf{a}$ and $\boldsymbol{\alpha}$ to be equal to zero. These three variations respectively yield to the state equation, the adjoint equation and the calibration condition:

$$\begin{cases} \dot{\mathbf{a}} = (\mathbf{A}_{\mathbf{rt}} + \mathbf{I}_{1+\alpha}\mathbf{A}_{\mathbf{rd}})\mathbf{a} + (\mathbf{B}_{\mathbf{rt}} + \mathbf{I}_{1+\alpha}\mathbf{B}_{\mathbf{rd}})\mathbf{u} \\ -\dot{\tilde{\mathbf{a}}} = {}^{t}(\mathbf{A}_{\mathbf{rt}} + \mathbf{I}_{1+\alpha}\mathbf{A}_{\mathbf{rd}})\tilde{\mathbf{a}} + 2(\mathbf{a}-\mathbf{b})\ ;\ \tilde{\mathbf{a}}(T) = \mathbf{0} \\ \boldsymbol{\alpha} = -\dfrac{1}{2\beta^2}\displaystyle\int_0^T {}^{t}(\mathbf{A}_{\mathbf{rd}} + \mathbf{B}_{\mathbf{rd}}\mathbf{u})\tilde{\mathbf{a}}dt \end{cases} \quad (14)$$

This system of coupled ordinary differential can be solved by a simple iterative process.

3. Application

3.1 Case study

This study deals with a 4.90 m × 2.82 m × 2.76 m room equipped with a fan coil having two outlet speeds (1 and 1.5 m/s) and an outlet temperature varying from 16 to 21 °C (Figure 1a). The fan coil is placed at the right bottom. Each wall temperature is considered homogeneous and constant.

The complete CFD model of this room is considered in 2D for computational time reasons. However, this 2D approach does not reduce the generality of the methodology proposed in this paper. A study on the application of POD to 3D CFD results obtained for a similar room showed that less than 10 eigenfunctions are needed to obtain a reliable reduce model (Basman et al 2005). It is worth mentioning that convergence of CFD model was difficult to achieve for an inlet temperature closed to 20 °C and a velocity of 1.0 m/s, certainly because of a physical transition in the flow pattern.

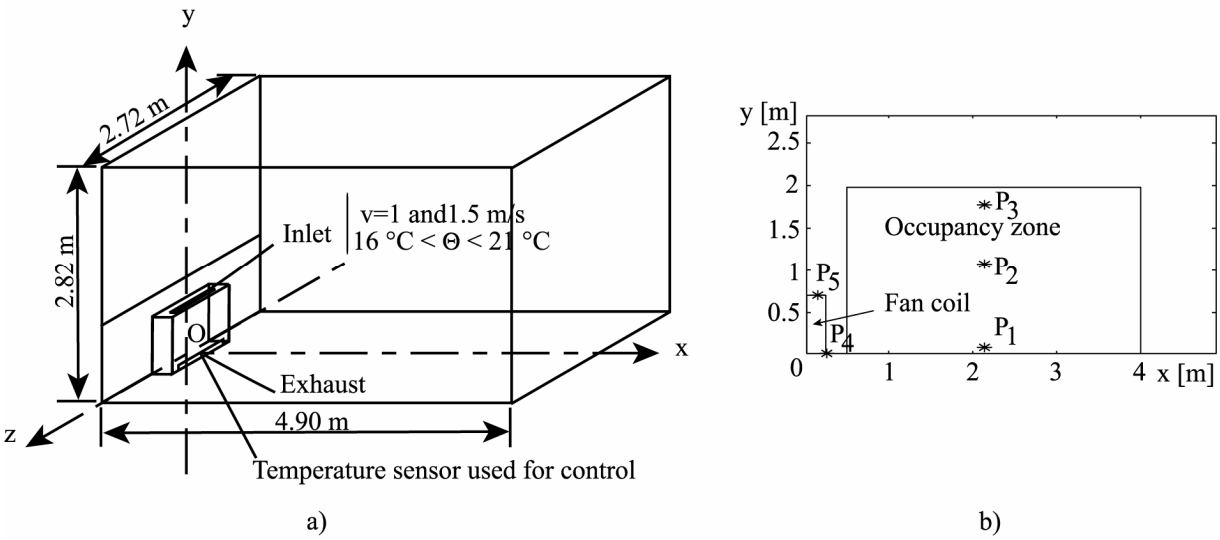

a) b)

Figure 1. View of the studied room: (a) 3D scheme and (b) 2D vertical mid plane (xOy).

In reference to the European standard EN ISO 7730 (1995), the control of temperature is surveyed at three different points in the occupancy zone, respectively at 0.10 m (P1), 1.10 m (P2) and 1.80 m (P3) high. In addition, the temperature at the inlet of the fan coil (P4) is checked. The location of these points on the vertical mid plane of the room is illustrated on Figure 1b.
In order to evaluate the accuracy of reduced models, we compare their results with CFD simulations and the root mean square error is used:

$$Rmse = \sqrt{\frac{\sum (\theta_{ref} - \theta)^2}{n_\theta}} \qquad (15)$$

Where n_θ is the number of cells for steady simulations, or number of time step for transient simulations.

3.2 Reduction of the state space model

In order to use the fixed velocity field, it is necessary to distinguish four different cases: a) jet falling before reaching the ceiling, b) jet sticking to the ceiling and falling rapidly, c) jet sticking to the ceiling and falling before the opposite wall, d) jet flow sticking to the ceiling and reaching the opposite wall. Figure 2 gives an illustration of these 4 cases. Each one can be defined by a range of outlet temperature and an outlet velocity (Table 1). The methodology described in the previous section is applied to each case.
At first, the accuracy of the four high order models has to be checked. It is interesting to have a closer look to case c) which is the less advantageous because of the behaviour of the jet. Indeed, the jet is developing quickly along the ceiling without reaching the opposite wall. The accordance with the fixed flow hypothesis is worse than for the other cases. Figure 3 shows the difference of temperature distribution for an outlet temperature of 21 °C and a temperature step of 1°C. The *Rmse* is equal to 0.240 °C for the whole room, 0.205 °C in the

Table 1. Parameters of the cases

	Outlet temperature [°C]	Outlet velocity [m/s]
Case a	16.0 to 16.7	1.0
Case b	16.7 to 19.7	1.0
Case c	19.7 to 21.0	1.0
Case d	16.0 to 21.0	1.5

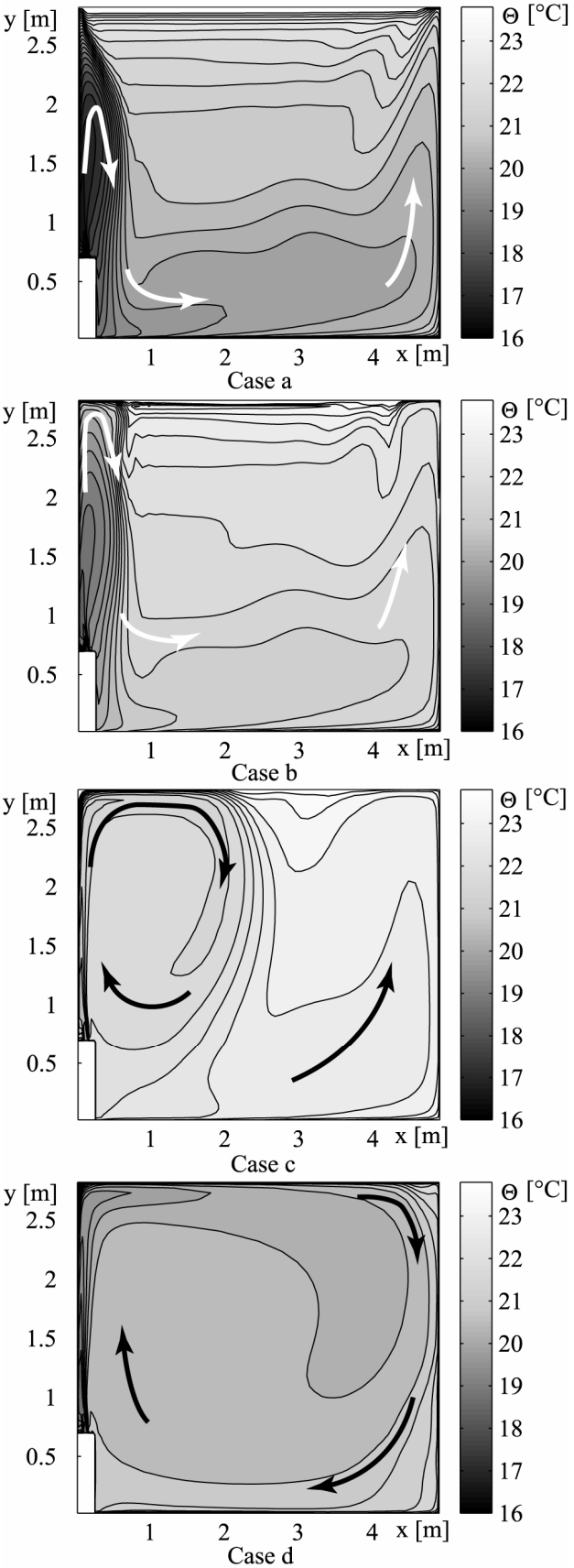

Figure 2. Studied cases

occupancy zone and 0.017 °C at the inlet of the fan coil. For all the room, the value is higher because of the difficulty in forecasting the jet flow correctly. The same remark is also valid for the steady state at 20 °C, where the jet flow largely enters in the occupancy zone (Figure 3a) and results in a *Rmse* of 0.420 °C in this zone. Nevertheless, the study of the transient period (Figure 4) shows that only points placed in high gradient zone undergo such error (*Rmse*=0.439 °C at P2), whereas points P1 and P3 have *Rmse* equal to 0.154 °C and 0.170 °C respectively. The simulations of the high order model only spend a few minutes whereas CFD simulations need several hours. However this computed time are still too long for real time control. Besides, the order of the model (2992) has to be reduced again to allow the construction of a controller.

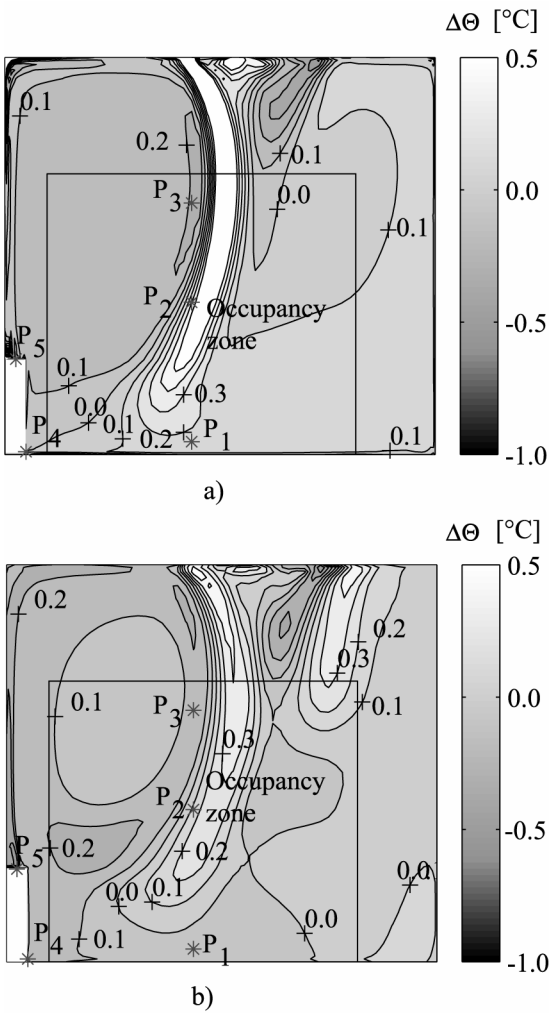

Figure 3. Difference of temperature for the case c) and for an outlet temperature of 21 °C between: (a) the high order model and full CFD model, (b) the reduced order model and full CFD model.

The POD-based basis functions are extracted from the simulation results of two opposite successive steps of outlet temperature describing all the range of each configuration. For instance and for the case c), 60 snapshots have been extracted from CFD simulations with a time step of 60 s (23 for the step from 19.7 to 21.0 °C and 37 for the step from 21.0 to 19.7 °C). They only contain the transient period of the temperature variation. Snapshots have been systematically extracted from CFD except for the case b). Indeed, because of the difficulty in

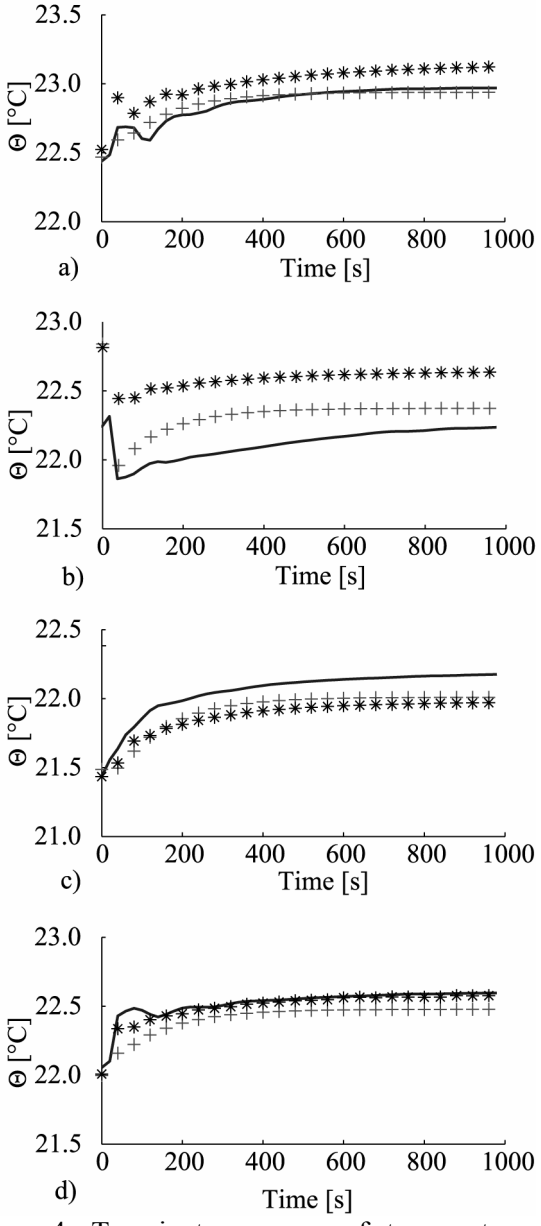

Figure 4. Transient response of temperature for the case c) and for an outlet temperature step from 20 at 21 °C at the point: (a) P1, (b) P2, (c) P3, (d) P4; temperature computed with CFD (solid line), the high order model (stared line) and the reduced order model (crossed line).

stabilizing the CFD simulation, the high order state space model is used to generate snapshots. For all cases, the cumulative contribution to the total "energy" is given in the last column of Table 2. Note that only a very few eigenfunctions are necessary to capture more than 90% of the "energy". The principal eigenfunction contributes at least 72% of the total "energy". The number of eigenfunctions needed in order to satisfy the criterion (5) is respectively 4, 3, 7 and 3 for case a) to d). Although it is not necessary to keep seven modes for all the cases, all the models are reduced to the same order 7.

Table 2. Eigenvalues of the eight most energetic modes and their contribution to the total temperature "energy".

Modes	Eigenvalues λ	Cumulative "energy" contribution E [%]
Case a		
1	0.2809	83.93
2	0.0439	97.05
3	0.544E-04	98.68
4	0.198E-04	99.27
5	0.102E-04	99.58
6	0.554E-05	99.74
7	0.222E-05	99.81
8	0.203E-05	99.87
Case b		
1	4.4437	84.98
2	0.7457	99.27
3	0.0287	99.82
4	0.0061	99.94
5	0.0022	99.98
6	0.747E-03	99.99
7	0.262E-03	100.00
8	0.834E-04	100.00
Case c		
1	0.7359	72.98
2	0.1367	86.54
3	0.0492	91.42
4	0.0393	95.32
5	0.0128	96.58
6	0.0077	97.35
7	0.0070	98.05
8	0.0054	98.58
Case d		
1	32.9710	98.15
2	0.5729	99.86
3	0.0234	99.93
4	0.0083	99.95
5	0.0081	99.98
6	0.0045	99.99
7	0.0011	99.99
8	0.707E-03	100.00

3.3 Calibration

Figures 5 to 8 compare the temporal coefficients obtained with the reduced state space system before calibration and after calibration to coefficients directly issued from the projection of the snapshot on the POD base.

For cases a) and d), the shape is similar for the first two coefficients but not for the others which is reasonable as more than 97% of the energy (Equation 5) is contained in the first two modes. For case a), the correction seems to be absolutely necessary to improve the forecast of the temporal coefficient. On the contrary, for the case d), the correction has a paradoxical effect because it decreases the precision of the model on the first two coefficients, which highlights a problem with the chosen method of correction. Indeed, the minimization of the cost functional led to the minimization of the overall gap between the temporal coefficients from the projection of snapshots and those calculated with the reduced state space model. So it is possible that some factors are improved while others are degraded while minimizing the functional. This is what happens in cases d), especially since seven modes are retained, while three would suffice. In conclusion, it was decided not to correct the model of case d), but it must be ascertained that the accuracy of the model is well enough.

At last, it is worth noticing that the coefficients are very close for the case b). The reduced state space model does not be dramatically improved by the calibration. Contrary to the three other cases, the snapshots are not obtained from CFD simulation but from the high order state space model. In the case of c), it must be emphasized that the correction has been little affected by the fluctuation of the second part of the temporal factors due to the difficulty in stabilizing CFD simulations.

Finally, this method not only allows calibration to correct the truncation errors, but also to take account of all the modeling errors. This remark makes sense to explain the difficulties to properly correct the case a), since the calibration also took into account the error made because of the assumption of a fixed velocity field.

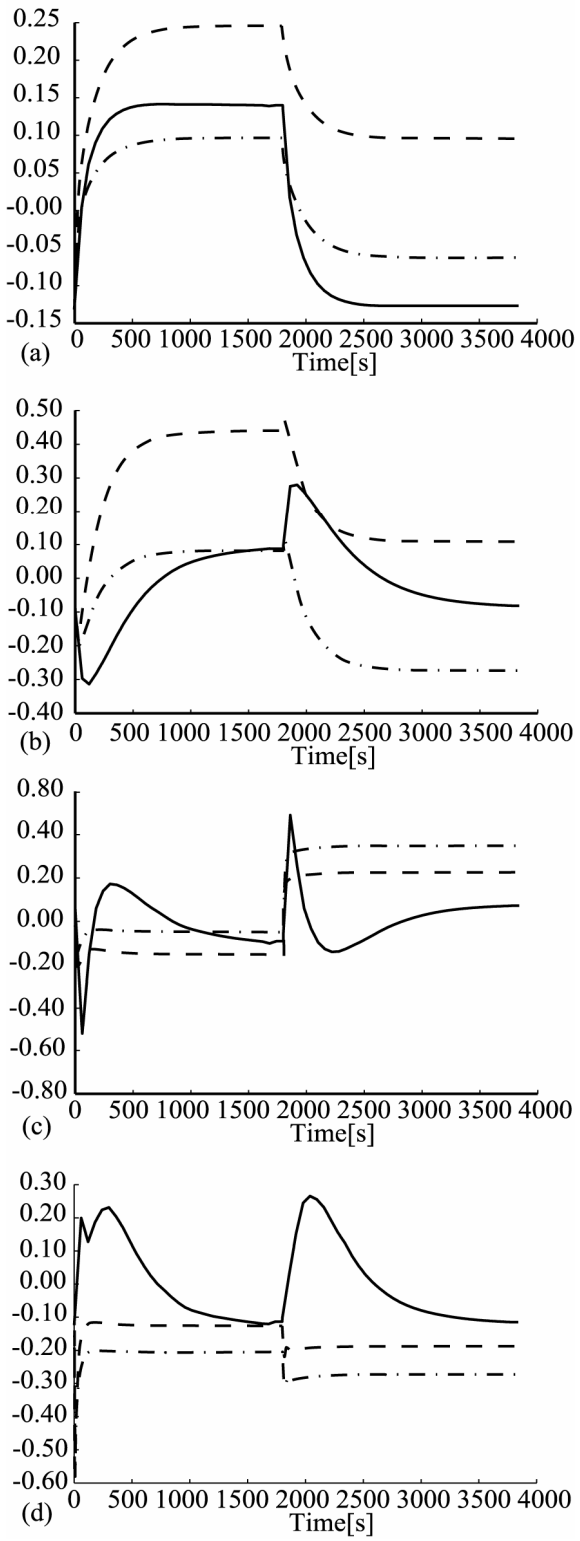

Figure 5. Temporal coefficients of the first four mode for the case a): (a) Mode 1, (b) Mode 2, (c) Mode 3, (d) Mode 4; coefficients directly issued from the projection of the snapshot on the POD base (solid line), obtained with the reduced state space system before calibration (dash line) and after calibration (dash dot line)

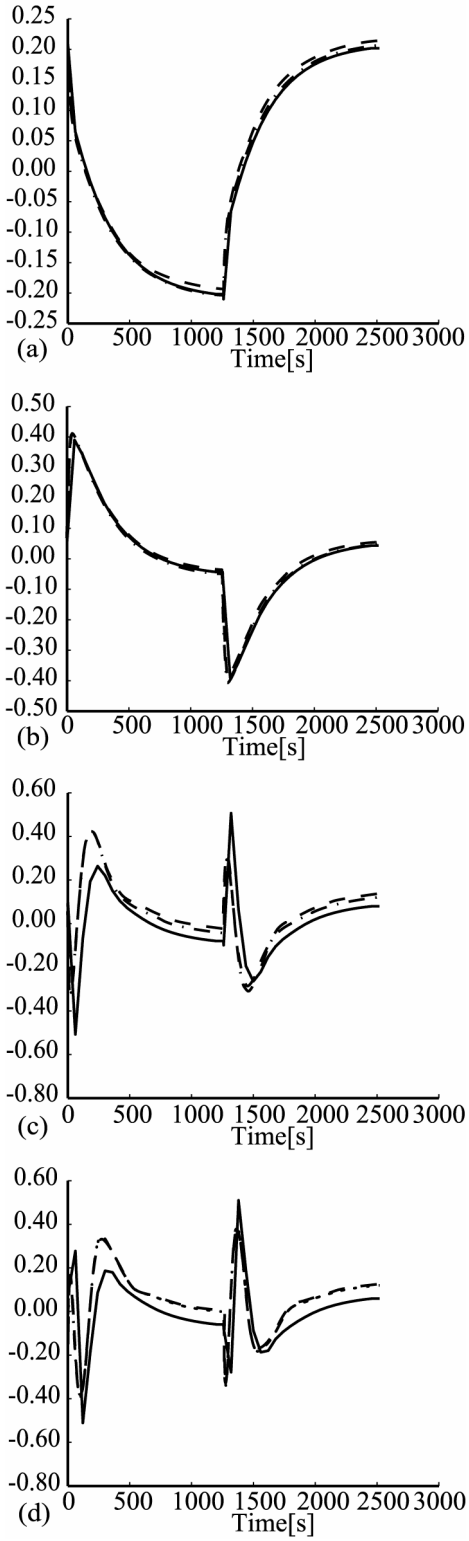

Figure 6. Temporal coefficients of the first four mode for the case b): (a) Mode 1, (b) Mode 2, (c) Mode 3, (d) Mode 4; coefficients directly issued from the projection of the snapshot on the POD base (solid line), obtained with the reduced state space system before calibration (dash line) and after calibration (dash dot line)

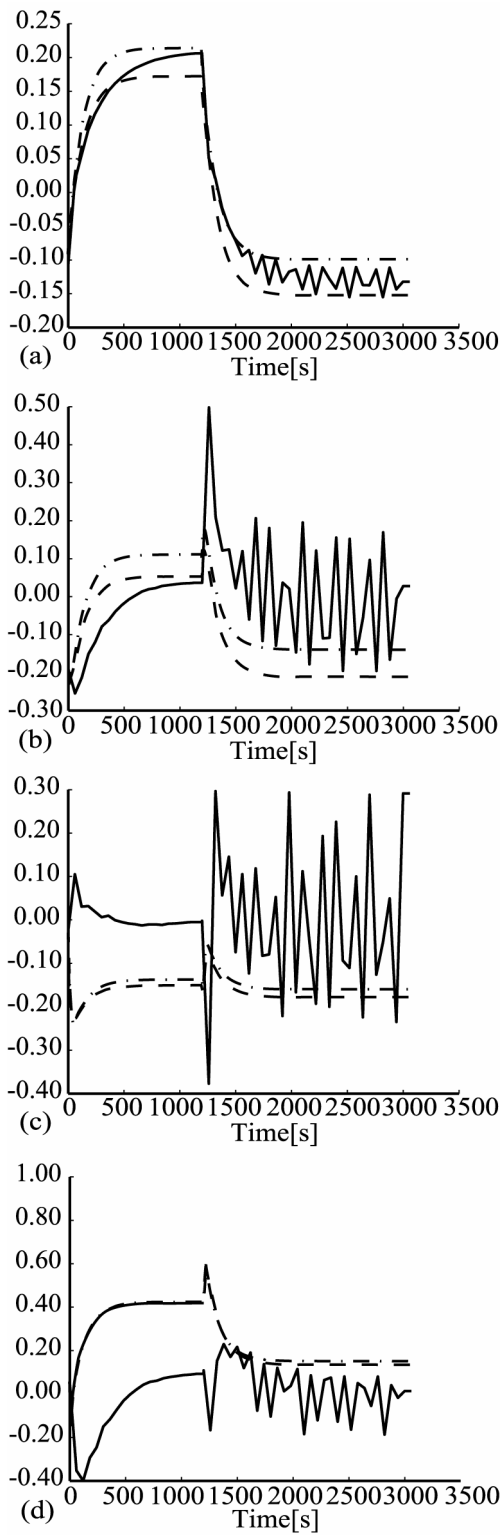

Figure 7. Temporal coefficients of the first four mode for the case c): (a) Mode 1, (b) Mode 2, (c) Mode 3, (d) Mode 4; coefficients directly issued from the projection of the snapshot on the POD base (solid line), obtained with the reduced state space system before calibration (dash line) and after calibration (dash dot line)

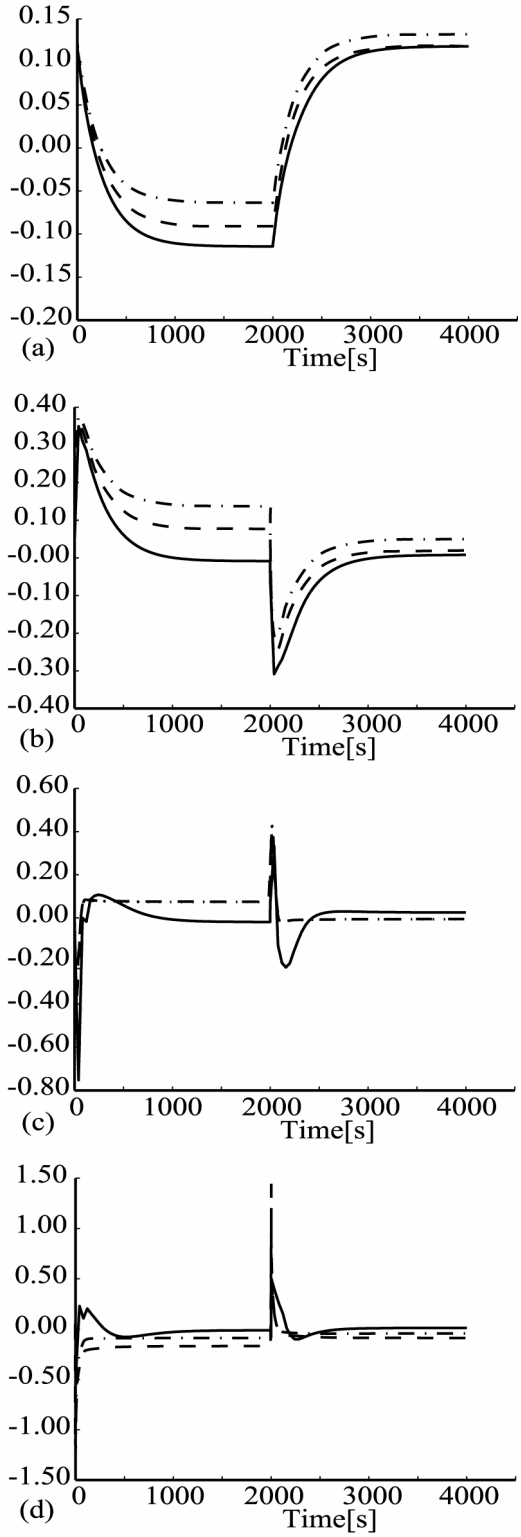

Figure 8. Temporal coefficients of the first four mode for the case d): (a) Mode 1, (b) Mode 2, (c) Mode 3, (d) Mode 4; coefficients directly issued from the projection of the snapshot on the POD base (solid line), obtained with the reduced state space system before calibration (dash line) and after calibration (dash dot line)

3.4 Comparison with CFD

Again, the case c) is chosen to consider the validation of the reduced order model. Comparing the simulation results of the reduced order model with the full CFD model, it results that the reduction does not systematically reduce the accuracy (Figure 3b). In the case of an outlet temperature of 20 °C for instance, the steady state *Rmse* decreases at 0.317 °C in the working zone. For the steady state at 21 °C, the accuracy of the reduced order model (Figure 3b) is increased at 0.152 °C and 0.124 °C for respectively all the room and the working zone, and it is decreased for the inlet of the fan coil at 0.127 °C, which remains acceptable. Concerning the transient period, results are better than high order model ones, above all for the point P2 (Figure 4b) with a *Rmse* of 0.229 °C. It is worth remembering that the base of reduction is built without the hypothesis of fixed flow field. Consequently, the base contains information on the velocity field variation, and so enhances the reduced order model compared to the higher order model.
For all cases, not only the accuracy is good, but resolution is made in real time. In addition, the size of the reduced order model is only 7, which allows controller design.

4. Conclusions

These results show a good capacity of reduced models obtained with Proper Orthogonal Decomposition (POD) to predict the temperature in the occupancy zone. Two solutions exist in order to generate the snapshots needed for the reduction respectively based on the full CFD model and on the high order sate space model. The choice depends on both the quality of CFD simulations and the results of the state space model. However, the decision will have a significant impact on the efficiency or the difficulty of calibrating the reduced order model necessary to take into account the truncation errors in the second case, but also errors of the high order model in the first.
Last but not least, the small size of these models allows real time applications such as the controller design for air temperature in indoor spaces. Besides, the use of state space form is suited to the application of modern control theory.

References

EN ISO 7730: Ergonomics of the thermal environment - Analytical determination and interpretation of thermal comfort using calculation of the PMV and PPD indices and local thermal comfort criteria. (1995).

Allery C. (2002) "Contribution à l'identification des bifurcations et à l'étude des écoulements fluides par des systèmes dynamiques d'ordre faible (P.O.D.)", Thesis, Poitiers. pp 184.

Allery C, Beghein C and Hamdouni A. (2005) "Applying proper orthogonal decomposition to the computation of particle dispersion in a two-dimensional ventilated cavity", Communication in Nonlinear Science and Numerical Simulation. 2005 10 pp 907-920.

Basman E and Khalifa E H. (2005) "Application of proper orthogonal decomposition to indoor airflows", ASHRAE Transactions. 2005 111 pp 625-634.

Couplet M, Sagaut P and Basdevant C. (2003) "Intermodal energy transfers in a proper orthogonal decomposition-Galerkin representation of a turbulent separated flow." Journal of Fluid Mechanics. 2003 Volume 491 pp 275-284.

Deane A E and Sirovich L. (1991) "A computational study of Rayleigh-Bénard convection. Part 1. Rayleigh-number scaling", Journal of Fluid Mechanics. 1991 222 pp 231-250.

Ghiaus C and Ghiaus A G. (1999) "Evaluation of the indoor temperature field using a given air velocity distribution", Building and Environment. 1999 34 pp 671-679.

Gunes H. (2002) "Low-order dynamical models of thermal convection in high-aspect ratio enclosures", Fluid Dynamics Research. 2002 30 pp 1-30.

Peng X. (1996) "Modeling of indoor thermal conditions for comfort control in buildings", PHD Thesis, Delft university of technology. pp 158.

Podvin B and Le Quere P. (2001) "Low-order models for the flow in a differentially heated cavity", Physics of Fluids. 2001 13 pp 3204-3214.

Rempfer D. (1994) "On the structure of dynamical system describing the evolution of coherent structures in a convective boundary layer", Physics of fluids. 1994 6 pp 1402-1404.

Sirovich L. (1987) "Turbulence and the dynamics of coherent structures, Part 1 : Coherent structures. Part 2 : Symmetries and transformations. Part 3 : Dynamics and scaling", Quarterly of Applied Mechanics. 1987 45 pp 561-590.